

Low-temperature galvanomagnetic transport of the two-dimensional electron gas in GaAs quantum wells

P. K. Ghosh and D. Chattopadhyay

Institute of Radiophysics and Electronics, University of Calcutta, 92, Acharya Prafulla Chandra Road, Calcutta 700 009, India

(Received 17 June 1993)

Hall mobility, Hall-to-drift mobility ratio, and the magnetoresistance coefficient of the two-dimensional (2D) electron gas in a square quantum well of GaAs are calculated in the temperature range 4–40 K in the framework of Fermi-Dirac statistics. Carrier scattering via screened deformation potential acoustic, piezoelectric, and ionized impurity interactions are considered. The variation of the galvanomagnetic coefficients is studied with lattice temperature, 2D carrier concentration, channel width, and the magnetic field in the classical region. Our calculated mobilities agree well with the available experimental data. The magnetoresistance coefficient is found to be quite sensitive to the change of the system parameters.

I. INTRODUCTION

Electronic transport properties of the two-dimensional (2D) electron gas in quantum wells are of considerable interest from both the physics and the device application points of view.¹ However, investigations of the galvanomagnetic coefficients of the 2D electron gas for classical magnetic fields are scarce in the literature. In an earlier paper,² we studied the galvanomagnetic transport of the 2D electrons in GaAs square quantum wells considering polar-optic and acoustic-phonon interactions. Similar studies at low temperatures are important, since the reduction of phonon scattering and the suppression of impurity scattering due to modulation doping enhance mobilities.³ Also, low temperatures are preferred to reduce the noise and the energy spread of electrons involved in transport.⁴ In this paper, we calculate the Hall mobility, Hall-to-drift mobility ratio, and the magnetoresistance coefficient of the 2D electron gas in a GaAs square quantum well in the temperature range 4–40 K where interactions with acoustic phonons via deformation potential and piezoelectric couplings and with ionized impurities are important. The effects of the 2D carrier concentration, channel width, and the magnetic field on the galvanomagnetic coefficients are studied. Our calculated mobilities are found to agree with the experimental data.^{5–8}

II. THEORY

We consider a square quantum well with infinite barrier height and of width L . Over the range of temperature, the channel width, and the 2D carrier concentration considered here, the separation between the first excited state and the ground quantum state is found to be at least five times the Fermi level. Consequently, the carriers are assumed to populate only the ground quantum state. Electron scattering via deformation potential acoustic, piezoelectric, and background impurities is considered including screening. Theoretical treatments of far remote impurity scattering in modulation-doped systems are

inadequate.⁹ However, for sufficiently thick spacers, the effect of the far remote impurities is negligibly small,¹⁰ and is therefore not considered here.

We set up a rectangular Cartesian coordinate system with the z axis perpendicular to the interfacial planes so that the electron gas is confined to move parallel to the xy plane. The electric field \mathcal{E} and the magnetic field \mathbf{B} are assumed to be along the x and the z axes, respectively. The carrier distribution function is written as

$$f(\mathbf{k}) = f_0(E) - \left[\frac{e\hbar\mathcal{E}}{m^*} \right] \left[\frac{\partial f_0}{\partial E} \right] [k_x \zeta_x(E) - \omega_B k_y \zeta_y(E)], \quad (1)$$

where $f_0(E)$ is the equilibrium Fermi-Dirac distribution function, e is the magnitude of the electron charge, \hbar is Planck's constant divided by 2π , m^* is the electron effective mass, $\omega_B (=eB/m^*)$ is the cyclotron resonance angular frequency, and k_x, k_y are the components of the 2D wave vector \mathbf{k} along the x and y axes, respectively. $\zeta_x(E)$ and $\zeta_y(E)$ are the perturbation functions to be determined from the Boltzmann transport equation which gives

$$\tau^{-1}(E)\zeta_x(E) = 1 - \omega_B^2 \zeta_y(E) \quad (2)$$

and

$$\tau^{-1}(E)\zeta_y(E) = \zeta_x(E). \quad (3)$$

Here, $\tau(E)$ is the momentum relaxation time and is given by

$$\tau^{-1}(E) = \tau_{ac}^{-1}(E) + \tau_{pz}^{-1}(E) + \tau_{im}^{-1}(E), \quad (4)$$

where $\tau_{ac}(E)$, $\tau_{pz}(E)$, and $\tau_{im}(E)$ are, respectively, the momentum relaxation times for acoustic, piezoelectric, and ionized impurity scatterings. The detailed expressions for τ_{ac} and τ_{pz} are found in Ref. 11 while that for τ_{im} is given in Ref. 12. Equations (2) and (3) yield

$$\zeta_x(E) = \frac{\tau(E)}{1 + \omega_B^2 \tau^2(E)} \quad (5)$$

and

$$\zeta_y(E) = \tau(E) \zeta_x(E) . \quad (6)$$

The Hall mobility (μ_H), Hall ratio (r_H), and the magnetoresistance coefficient (R_m) are expressed by²

$$\mu_H = \frac{\mu_{xx}(0) |\mu_{xy}|}{B(\mu_{xx}^2 + \mu_{xy}^2)} , \quad (7)$$

$$r_H = \mu_H / \mu_{xx}(0) , \quad (8)$$

and

$$R_m = \frac{\mu_H \mu_{xx} B}{|\mu_{xy}|} - 1 , \quad (9)$$

where

$$\mu_{xx} = \frac{e}{\pi N_{2D} \hbar^2} \int_0^\infty E \frac{\tau(E)}{1 + \omega_B^2 \tau^2(E)} \left(-\frac{\partial f_0}{\partial E} \right) dE \quad (10)$$

and

$$\mu_{xy} = \frac{e \omega_B}{\pi N_{2D} \hbar^2} \int_0^\infty E \frac{\tau^2(E)}{1 + \omega_B^2 \tau^2(E)} \left(-\frac{\partial f_0}{\partial E} \right) dE . \quad (11)$$

In Eqs. (7) and (8), $\mu_{xx}(0)$ is the value of μ_{xx} for $B = 0$.

III. RESULTS AND DISCUSSIONS

Calculations are done with the following parameter values of GaAs: effective mass $m^* = 0.067 m_0$, acoustic deformation constant $E_1 = 11$ eV, longitudinal elastic constant $c_l = 14.03 \times 10^{10} \text{ N m}^{-2}$, transverse elastic constant $c_t = 4.864 \times 10^{10} \text{ N m}^{-2}$, static dielectric constant $K_0 = 12.53$, and piezoelectric tensor component $h_{14} = 1.44 \times 10^9 \text{ V m}^{-1}$. Although the commonly accepted value of E_1 is 7 eV, we use here a higher value of 11 eV which is obtained from the analysis of the energy-loss rates of the 2D electrons.¹³

Figures 1 and 2 show the temperature dependence of Hall mobility. The curves in Fig. 1 are calculated with the experimental parameter values, viz., channel width $L = 16.1$ nm and the 2D carrier concentration $N_{2D} = 1.64 \times 10^{15} \text{ m}^{-2}$; the points refer to the measured values of Guillemot *et al.*^{5,6} The curves in Fig. 2 are obtained with the experimental parameter values $L = 15$ nm and $N_{2D} = 2 \times 10^{15} \text{ m}^{-2}$; the points give the experimental values.^{7,8} The calculated results are found to agree with the experimental data for a typical value of $6 \times 10^{21} \text{ m}^{-3}$ for the ionized impurity concentration N_i . The curves in Figs. 1 and 2 are for a magnetic field $B = 0.02$ T. The Hall mobility μ_H is quite insensitive to a change in B : we find that as B is reduced to 0.005 T, μ_H changes by 1.2% only. Interestingly, the measured mobilities in the temperature range concerned here could not be explained by

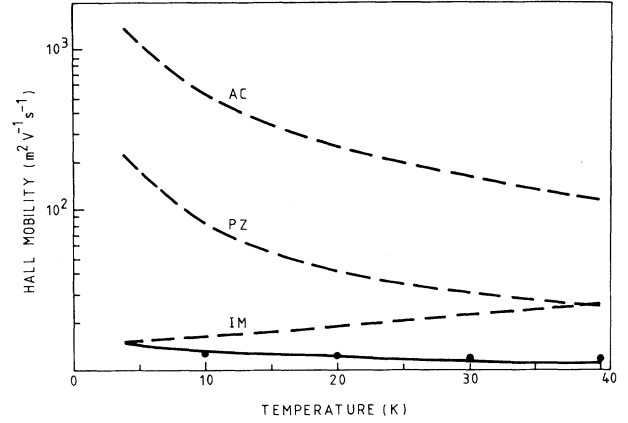


FIG. 1. Hall mobility vs lattice temperature for $L = 16.1$ nm, $N_{2D} = 1.64 \times 10^{15} \text{ m}^{-2}$, $N_i = 6 \times 10^{21} \text{ m}^{-3}$, and $B = 0.02$ T. The curves marked AC, PZ, and IM represent, respectively, the Hall mobilities due to deformation potential acoustic, piezoelectric, and ionized impurity interactions. The solid curve gives the overall mobility due to all the scattering mechanisms. The points show experimental results (Refs. 5 and 6).

Leon, Leon, and Comas¹⁴ considering phonon scattering only.

The mobilities limited by deformation potential acoustic and piezoelectric scattering are seen to decrease with the increase of lattice temperature due to the reduction of the phonon occupation numbers. However, the ionized impurity-limited mobility increases with temperature owing to its Coulombic nature. The overall mobility decreases slowly with the increase in lattice temperature and is dominated by ionized impurity scattering in the low-temperature regime.

Figure 3 depicts the variation of the Hall-to-drift mobility ratio with the lattice temperature for the parameter values of Figs. 1 and 2. At very low temperatures, the 2D electron gas is strongly degenerate so that the Hall-

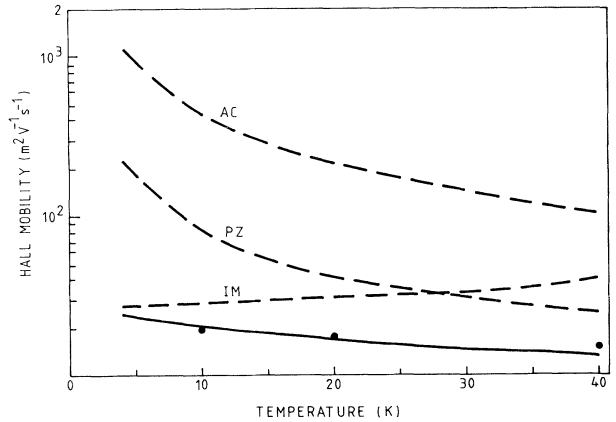


FIG. 2. Hall mobility vs temperature for $L = 15$ nm, $N_{2D} = 2 \times 10^{15} \text{ m}^{-2}$, $N_i = 6 \times 10^{21} \text{ m}^{-3}$, and $B = 0.02$ T. The curves have the same significance as in Fig. 1. The points give the experimental values (Refs. 7 and 8).

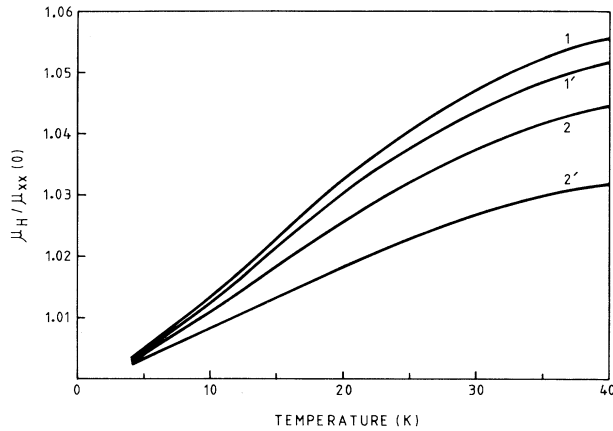


FIG. 3. Hall-to-drift mobility ratio $\mu_H/\mu_{xx}(0)$ vs lattice temperature. (1), (1'): $L = 16.1$ nm, $N_{2D} = 1.64 \times 10^{15} \text{ m}^{-2}$; (2), (2'): $L = 15$ nm, $N_{2D} = 2 \times 10^{15} \text{ m}^{-2}$. The unprimed curves are for $B = 0.005$ T and the primed curves are for $B = 0.02$ T.

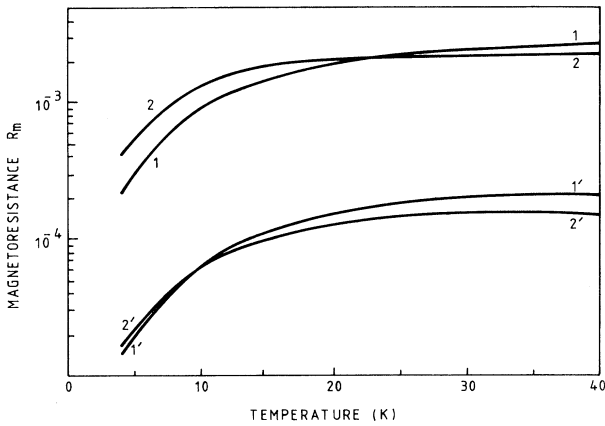


FIG. 4. Magnetoresistance vs lattice temperature. The labels of the curves have the same significance as in Fig. 3.

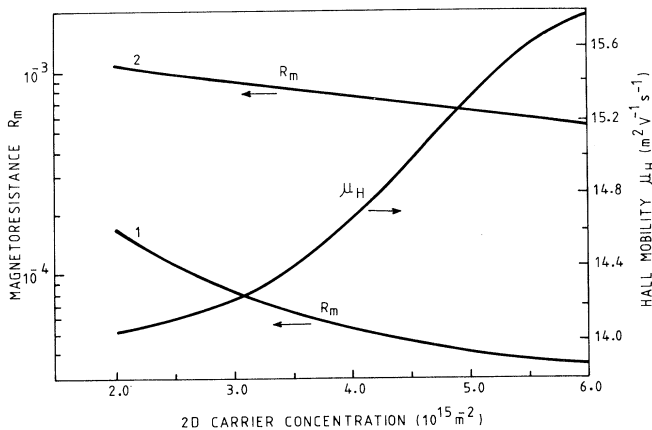


FIG. 5. Magnetoresistance and Hall mobility against 2D carrier concentration for $L = 10$ nm, $T = 30$ K, and $N_i = 6 \times 10^{21} \text{ m}^{-3}$. (1) $B = 0.005$ T; (2) $B = 0.02$ T.

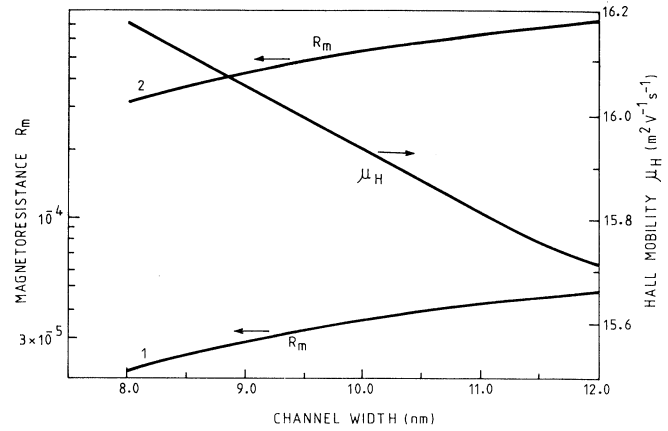


FIG. 6. Magnetoresistance and Hall mobility against channel width for $T = 30$ K, $N_i = 6 \times 10^{21} \text{ m}^{-3}$, and $N_{2D} = 6 \times 10^{15} \text{ m}^{-2}$. (1) $B = 0.005$ T; (2) $B = 0.02$ T.

to-drift mobility ratio is quite close to unity. The ratio increases with temperature as the degeneracy of the system decreases. For a fixed temperature, the ratio is found to decrease with an increase of the magnetic field. The Hall mobility deviates from the drift mobility by less than 6%, so that the replacement of the Hall mobility by the drift mobility does not generally introduce large errors.

The variation of the magnetoresistance coefficient (R_m) with the lattice temperature for parameter values of Figs. 1 and 2 is shown in Fig. 4. The magnetoresistance coefficient decreases at very low temperatures where the system is markedly degenerate. R_m is found to be very sensitive to changes in the magnetic induction B : as B is increased from 0.005 to 0.02 T, R_m increases by an order of magnitude. Experimental results on R_m for the 2D systems for classical fields are, however, not yet available for a comparison with our calculations.

Figures 5 and 6, respectively, give the variation of R_m and μ_H with the 2D carrier concentration (N_{2D}) and the channel width (L) for a lattice temperature (T) of 30 K for which R_m is large. A typical value of $6 \times 10^{21} \text{ m}^{-3}$ is assumed for the ionized impurity concentration (N_i) for these figures. Figure 5 shows that μ_H increases and R_m decreases with increasing N_{2D} . The enhanced screening of the scattering rates with increasing N_{2D} explains these results.^{11,12} But as L increases, the phonon scattering is weaker¹¹ and the impurity scattering gets stronger,¹² forcing μ_H to fall and R_m to rise (see Fig. 6). Interestingly, R_m is more sensitive than μ_H to the changes in system parameters like L and N_{2D} and also to changes in B . Thus the measurements of R_m would throw more light on the carrier kinetics in quantum wells.

ACKNOWLEDGMENT

One of us (P.K.G.) is grateful to the Council of Scientific and Industrial Research, India, for financial support.

- ¹J. J. Harris, J. A. Pals, and R. Woltjer, *Rep. Prog. Phys.* **52**, 1217 (1989).
- ²P. K. Ghosh, D. Chattopadhyay, A. Ghosal, and B. G. Mulumani, *Phys. Status Solidi B* **176**, 451 (1993).
- ³H. L. Stormer, *J. Phys. Soc. Jpn. Suppl. A* **49**, 1013 (1980).
- ⁴S. Datta and M. J. Mclellan, *Rep. Prog. Phys.* **53**, 1003 (1990).
- ⁵C. Guillemot, M. Baudet, M. Gauneau, A. Regreny, and J. C. Portal, *Superlatt. Microstruct.* **2**, 445 (1986).
- ⁶C. Guillemot, M. Baudet, M. Gauneau, A. Regreny, and J. C. Portal, *Phys. Rev. B* **35**, 2799 (1987).
- ⁷G. Weimann and W. Schlapp, *Appl. Phys. A* **37**, 139 (1985).
- ⁸H. Burkhard, W. Schlapp, and G. Weimann, *Surf. Sci.* **174**, 387 (1986).
- ⁹B. K. Ridley, *Semicond. Sci. Technol.* **3**, 111 (1988).
- ¹⁰J. J. Harris, C. T. Foxon, D. E. Lacklison, and K. W. J. Barnham, *Superlatt. Microstruct.* **2**, 563 (1986).
- ¹¹D. Chattopadhyay, *Phys. Status Solidi B* **135**, 409 (1986).
- ¹²J. Lee, H. N. Spector, and V. K. Arora, *J. Appl. Phys.* **54**, 6995 (1983).
- ¹³K. Hirakawa and H. Sakaki, *Appl. Phys. Lett.* **49**, 889 (1986).
- ¹⁴H. Leon, F. Leon, and F. Comas, *Phys. Status Solidi B* **170**, 449 (1992).